Data Enhanced Hierarchical Control to Improve Distribution Voltage with Extremely High PV Penetration

Preprint

Fei Ding, Harsha V. Padullaparti, Murali Baggu, Santosh Veda, and Shazreen Meor Danial

National Renewable Energy Laboratory

Presented at the 2019 IEEE Power & Energy Society General Meeting (IEEE PES GM)
Atlanta, Georgia
August 4–8, 2019

NREL is a national laboratory of the U.S. Department of Energy
Office of Energy Efficiency & Renewable Energy
Operated by the Alliance for Sustainable Energy, LLC

This report is available at no cost from the National Renewable Energy Laboratory (NREL) at www.nrel.gov/publications.

Contract No. DE-AC36-08GO28308

Conference Paper
NREL/CP-5D00-72755
September 2019

Data Enhanced Hierarchical Control to Improve Distribution Voltage with Extremely High PV Penetration

Preprint

Fei Ding, Harsha V. Padullaparti, Murali Baggu, Santosh Veda, and Shazreen Meor Danial

National Renewable Energy Laboratory

Suggested Citation
Ding, Fei, Harsha V. Padullaparti, Murali Baggu, Santosh Veda, and Shazreen Meor Danial. 2019. *Data Enhanced Hierarchical Control to Improve Distribution Voltage with Extremely High PV Penetration: Preprint*. Golden, CO: National Renewable Energy Laboratory. NREL/CP-5D00-72755. https://www.nrel.gov/docs/fy19osti/72755.pdf.

NREL is a national laboratory of the U.S. Department of Energy
Office of Energy Efficiency & Renewable Energy
Operated by the Alliance for Sustainable Energy, LLC

This report is available at no cost from the National Renewable Energy Laboratory (NREL) at www.nrel.gov/publications.

Contract No. DE-AC36-08GO28308

Conference Paper
NREL/CP-5D00-72755
September 2019

National Renewable Energy Laboratory
15013 Denver West Parkway
Golden, CO 80401
303-275-3000 • www.nrel.gov

NOTICE

This work was authored by the National Renewable Energy Laboratory, operated by Alliance for Sustainable Energy, LLC, for the U.S. Department of Energy (DOE) under Contract No. DE-AC36-08GO28308. Funding provided by U.S. Department of Energy Office of Energy Efficiency and Renewable Energy Solar Energy Technologies Office. The views expressed herein do not necessarily represent the views of the DOE or the U.S. Government. The U.S. Government retains and the publisher, by accepting the article for publication, acknowledges that the U.S. Government retains a nonexclusive, paid-up, irrevocable, worldwide license to publish or reproduce the published form of this work, or allow others to do so, for U.S. Government purposes.

Cover Photos by Dennis Schroeder: (clockwise, left to right) NREL 51934, NREL 45897, NREL 42160, NREL 45891, NREL 48097, NREL 46526.

Data-Enhanced Hierarchical Control to Improve Distribution Voltage with Extremely High PV Penetration

Fei Ding, *Senior Member, IEEE*, Harsha V. Padullaparti, *Member*, *IEEE*, Murali Baggu, *Senior Member*, *IEEE*, Santosh Veda, *Senior Member, IEEE*, Shazreen Meor Danial, *Member, IEEE*

National Renewable Energy Laboratory
15013 Denver W Pkwy, Golden, CO, 80401

***Abstract* — Dynamic, scalable, and interoperable control paradigms are required to enable efficient, secure, reliable, and resilient distribution grid operations with widespread grid integration of renewable energy resources. This paper presents our recent research on developing a novel, holistic, data-enhanced hierarchical control architecture that addresses the formidable challenges faced by emerging distribution grids with increasing penetrations of distributed energy resources. The proposed architecture integrates centralized monitoring and control with distributed grid-edge control and thus effectively deals with multi-spatiotemporal dynamics existing in the grid. Simulation results are provided to demonstrate the effectiveness of the proposed control architecture.**

***Index Terms* — distributed PV, voltage regulation, grid-edge control, advanced distribution management system.**

I. Introduction

The proliferation of distributed photovoltaic (PV) is creating operational challenges for the distribution grid, such as reverse power flows, transients from the variability of PV systems [1], feeder load balancing, and voltage stability [2]. These issues are exposing the weaknesses of existing distribution grid operations and controls including, but not limited to, lack of grid situational awareness, heuristic and slow-acting control actions, latency of control for emergency situations, and points of failure in communications. ANSI C84.1 standard [3] is enforced at the low-voltage service entrance (i.e., at the edge of the grid), and it requires range A voltage to stay within ±5% deviation from the nominal value. However, increasing PV penetration levels could boost voltage to exceed the ANSI limit and cause high-voltage variability and flicker because of solar intermittency. These issues call for new control paradigms that can comprehensively pave the way to next-generation electric grid settings where the massive integration of solar energy is operated with reliability and efficiency guarantees. To this end, control architectures are envisioned to leverage a hybrid approach whereby the speed and reliability of distributed control is coupled with the situational awareness and flexibility offered by centralized monitoring and control systems, such as an advanced distribution management system (ADMS). However, given the diversity of technologies and vendors as well as the competitiveness of the grid-edge marketplace, implementing monitoring and control solutions that are interoperable and cooperate to achieve the common goal of a reliable system-wide operation is a significant challenge. As a result, this paper describes our recent research on developing a novel, holistic, data-enhanced hierarchical control (DEHC) architecture that comprehensively addresses the formidable challenges faced by emerging distribution grids with increasing penetration levels of distributed renewable energy resources.

This work was authored by the National Renewable Energy Laboratory, managed and operated by Alliance for Sustainable Energy, LLC for the U.S. Department of Energy (DOE) under Contract No. DE-AC36-08GO28308. Funding provided by the U.S. Department of Energy Office of Energy Efficiency and Renewable Energy Solar Energy Technologies Office. The views expressed in the article do not necessarily represent the views of the DOE or the U.S. Government. The U.S. Government retains and the publisher, by accepting the article for publication, acknowledges that the U.S. Government retains a nonexclusive, paid-up, irrevocable, worldwide license to publish or reproduce the published form of this work, or allow others to do so, for U.S. Government purposes.

II. DEHC Architecture

The proposed DEHC architecture involves the development and the systematic integration of:

- Advanced applications for real-time operation and control (including centralized volt/volt-ampere reactive [VAR] optimization extended with generation control) of traditional volt/VAR resources (i.e., load-tap changers [LTCs], voltage regulators, capacitor banks) and edge devices (i.e., controllable devices at secondary circuits) offering reactive and active power support
- Real-time monitoring and forecasting of the distribution grid to gain comprehensive situational awareness and support the control decisions offered by DEHC
- Planning applications to provide what-if feasibility analysis for the connection of an increasing amount of distributed solar generation and dynamic assessments of the maximum amount of installed PV power without voltage violations and overloads.

As shown in Fig. 1, the DEHC architecture comprises three essential parts: a centralized volt-VAR-watt optimization

(VVWO) using ADMS, distributed PV inverter control based on real-time optimal power flow (RT-OPF), and grid-edge voltage regulation. Based on real-time supervisory control and data acquisition (SCADA) measurements, ADMS VVWO is able to directly control legacy voltage-regulating devices—e.g., LTCs, voltage regulators, and switchable capacitor banks—and provide voltage reference signals to manage grid-edge voltage-regulation devices and distributed PV inverters. Both grid-edge voltage-regulation device and distributed PV inverters are located at secondary circuits, and they can manage the low-voltage service voltages at grid edges. In our study, the ADMS system is developed by Schneider Electric [4], and the grid-edge voltage-regulation device is the Edge of Network Grid Optimizer (ENGO) device developed by Varentec [5], [6], which can automatically alter its reactive power injection into the grid based on the voltage reference signal received from ADMS. The active and reactive power outputs of distributed PV inverters are solved using the real-time optimal power flow model developed by the team to mitigate voltage violations and improve power quality. Communications between ADMS and external software and scripts follows the practical industry standard using DNP3 protocol. Details about all three DEHC components and control time coordination are provided next.

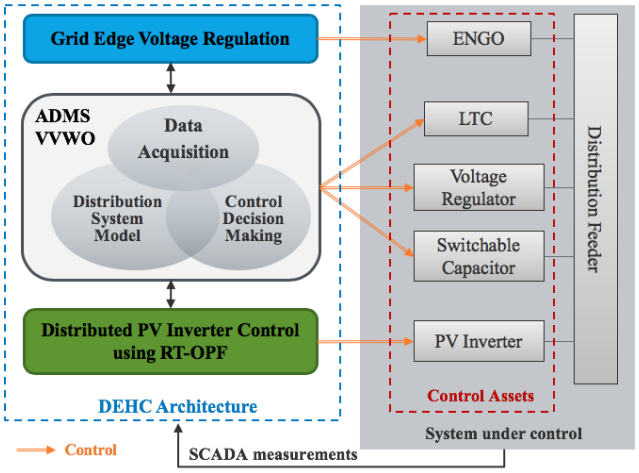

Fig. 1. Description of DEHC architecture.

A. Centralized Volt-VAR-Watt Control

The ADMS VVWO developed by Schneider authors is an integrated solution that manages voltages and reactive power flows in the distribution network. The application determines the optimal voltage control strategy to achieve the specified operating objective within the operating constraints. Some example applications include:

- Levelized voltage profile for all customers along a feeder
- Substation VAR support, improved feeder power factor, and reduced line losses
- Conservation voltage reduction—energy savings
- Demand reduction—peak load shaving
- Fast voltage reduction during emergency conditions—avoiding load shedding.

To calculate the optimal state, the ADMS VVWO supports both a model-based approach that solves its optimal decisions based on the estimated actual network state acquired from a state estimation algorithm and rule-based approaches that rely only on the ordering of devices to be controlled. The value of the model-based solution is that all decisions are based on the current state of the network instead of some assumed state. The initial state for the VVWO calculation is the current "as operated" network state with actual statuses and parameters of all control devices. In this way, the result of the VVWO calculation achieves a network state "better" (from the point of view of the optimization objective) than the current one, with minimal execution time (i.e., a minimal number of switching operations).

Depending on the final goal, the volt/VAR optimization can be stated as a simple optimization problem, with one objective only, but also as a very complex optimization problem, with several, sometimes contradictory objectives. The complexity of the problem lies in the fact that the solution of the considered problem depends on both planned and unplanned factors—e.g., loads depend on network voltages, loads and network topology vary in time, power losses depend on loads and network voltages, local automation significantly affects the problem, the value of real power injected in the distribution network by distributed generators depends on control laws that are applied on the considered distributed generators.

B. Grid-Edge Voltage Regulation

The ENGO device is paired with a grid-edge management system (GEMS) that can receive voltage reference signals from ADMS and send these signals to all ENGO devices at grid edge. Thus, the voltage reference signals are updated whenever ADMS VVWO is executed. ENGO/GEMS provides volt/VAR control capability at secondary distribution circuits. Based on the voltage reference signals, the ENGO device monitors its local terminal voltage and provides dynamic reactive power injection into the grid to maintain voltage within the preferred operation range defined by the voltage reference signal and voltage deadband (e.g., 124 V +/- 0.5 V). The local response time of the ENGO device is subcycle.

C. Distributed PV Inverter Control

Based on the AC optimal power flow model proposed in [7], we have developed the RT-OPF algorithm for the DEHC architecture to control PV inverters in a distributed manner. The objective of the RT-OPF is to minimize active power curtailment and reactive power output for all controlled PV inverters, and it is formulated as:

$$\min_{p_j^t, q_j^t} f(\mathbf{x^t}) = \sum_{j=1}^{NPV} c_P \cdot \left(p_j^{t,max} - p_j^t\right)^2 + c_Q \cdot \left(q_j^t\right)^2 \quad (1)$$

where $\mathbf{x^t} = \{p_j^t, q_j^t,\ j = 1, \dots, NPV\}$, and p_j^t and q_j^t are actual active power output and reactive power output from the j^{th} PV inverter at time t. NPV is the total number of distributed PV inverters under control. $p_j^{t,max}$ is the maximum active power output that can be generated from the j^{th} PV inverter at time t. c_P and c_Q are constant coefficients, and typically $c_P \gg c_Q$.

PV inverter operation should follow the current industry practice, which is limiting the amount of VAR to be 44% of the inverter capacity to restrict inverter power factor higher

than 0.9. Further, all PV inverters are able to operate at night modes, so the inverter can still generate and absorb reactive power even when there is no active power output from the PV array. Thus, the feasible solution set for p_j^t and q_j^t is defined as:

$$\chi^t = \begin{cases} 0 \le p_j^t \le p_j^{t,max} \\ \left(p_j^t\right)^2 + \left(q_j^t\right)^2 \le S_j^2 \\ \left(q_j^t\right)^2 \le 0.44^2 \cdot S_j^2 \end{cases} \quad (2)$$

where S_j is the inverter size for the j^{th} PV inverter.

All node voltages in the distribution feeder should not exceed the ANSI limit and/or the voltage reference signals received from the ADMS VVWO, so the voltage constraint is formulated as:

$$\underline{v}^t \le |v_k^t| \le \overline{v}^t, \ \forall k \in N \quad (3)$$

where v_k^t is the voltage of the k^{th} node at time t, and $\underline{v}^t$ and $\overline{v}^t$ are the lower and upper voltage limits for the targeted operational range at time t. N is the total number of nodes (excluding slack bus nodes) in the feeder. $|\cdot|$ is the magnitude of a complex value.

The linear power flow model proposed in [8] is leveraged to solve voltages for the three-phase unbalanced distribution network. Complex voltages ($\mathbf{V}$) and voltage magnitudes ($|\mathbf{V}|$) for all the nodes excluding slack buses can be modeled as the linear functions of node power injections, as:

$$\mathbf{V} = \mathbf{\Phi_P} \cdot \mathbf{P_{bus}} + \mathbf{\Phi_Q} \cdot \mathbf{Q_{bus}} + \boldsymbol{\varphi} \quad (4)$$

$$|\mathbf{V}| = \mathbf{\Psi_P} \cdot \mathbf{P_{bus}} + \mathbf{\Psi_Q} \cdot \mathbf{Q_{bus}} + \boldsymbol{\omega} \quad (5)$$

where $\mathbf{P_{bus}}$ and $\mathbf{Q_{bus}}$ are, respectively, the active power injection vector and reactive power injection vector at the feeder nodes. $\mathbf{\Phi_P}$, $\mathbf{\Phi_Q}$, $\mathbf{\Psi_P}$, and $\mathbf{\Psi_Q}$ are power coefficient matrices for the linear power flow model; and $\boldsymbol{\varphi}$ and $\boldsymbol{\omega}$ are constant vectors.

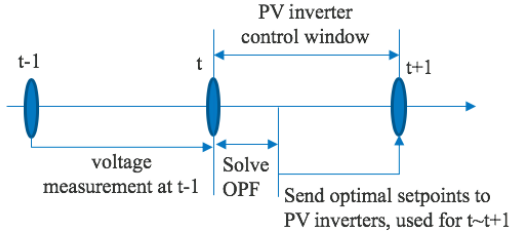

Fig. 2. Operation logic to solve the optimal power set points for PV inverters.

Then the primal dual gradient algorithm with voltage measurement as feedback is used to solve the problem following the online optimization principal. Fig. 2 shows the operation logic to solve the optimal power set points for the PV inverters. At the beginning of each control time window (t~t+1), the power set points ($\mathbf{x_t}$) for PV inverters are solved:

$$\mathbf{x_t} = \text{Proj}\left\{\mathbf{x_{t-1}} - \alpha_x \cdot \nabla_x \mathcal{L}(\mathbf{x_{t-1}}, \overline{\boldsymbol{\mu}}_{\mathbf{t-1}}, \underline{\boldsymbol{\mu}}_{\mathbf{t-1}})\right\} \quad (6)$$

And $\overline{\boldsymbol{\mu}}_{\mathbf{t-1}}$ and $\underline{\boldsymbol{\mu}}_{\mathbf{t-1}}$ are the Lagrangian multipliers for the upper and lower voltage limit constraints, respectively, and they are updated as:

$$\begin{cases} \overline{\boldsymbol{\mu}}_{\mathbf{t}} = \text{Proj}\left\{\overline{\boldsymbol{\mu}}_{\mathbf{t-1}} + \alpha_{\bar{\mu}} \cdot \nabla_{\bar{\mu}} \mathcal{L}(\hat{\mathbf{v}}_{\mathbf{t-1}} | \mathbf{x_{t-1}})\right\} \\ \underline{\boldsymbol{\mu}}_{\mathbf{t}} = \text{Proj}\left\{\underline{\boldsymbol{\mu}}_{\mathbf{t-1}} + \alpha_{\underline{\mu}} \cdot \nabla_{\underline{\mu}} \mathcal{L}(\hat{\mathbf{v}}_{\mathbf{t-1}} | \mathbf{x_{t-1}})\right\} \end{cases} \quad (7)$$

where $\alpha_x, \alpha_{\bar{\mu}}, \alpha_{\underline{\mu}}$ are constant stepsizes. $\nabla_x \mathcal{L}$, $\nabla_{\bar{\mu}} \mathcal{L}$, $\nabla_{\underline{\mu}} \mathcal{L}$ are the projected gradients and can be computed from (1)–(5); $\nabla_{\bar{\mu}} \mathcal{L}$ and $\nabla_{\underline{\mu}} \mathcal{L}$ are computed directly based on voltage measurements at last time ($\hat{\mathbf{v}}_{\mathbf{t-1}}$); $\nabla_x \mathcal{L}$ depends on $\mathbf{x_{t-1}}, \overline{\boldsymbol{\mu}}_{\mathbf{t-1}}, \underline{\boldsymbol{\mu}}_{\mathbf{t-1}}$, and it also depends on the power coefficient matrices of the linear power flow model.

D. Coordination of DEHC Components

Three control timescales exist in the DEHC architecture: 1) slow timescale (such as approximately 5–15 minutes)—the ADMS monitors the entire feeder based on real-time SCADA measurements and controls legacy voltage-regulating devices in a slow timescale, and it can also send reference signals for controllable grid-edge devices at the same timescale; 2) moderate timescale (such as approximately 1–60 seconds)—the RT-OPF solves the optimal power set points for PV inverters every several seconds to address the impact of solar intermittency on distribution voltage; 3) fast timescale (milliseconds)—the reactive power output from the ENGO devices at the grid edge are adjusted every few milliseconds based on the reference voltage signals received from the ADMS. Fig. 3 shows the coordination among the three control timescales.

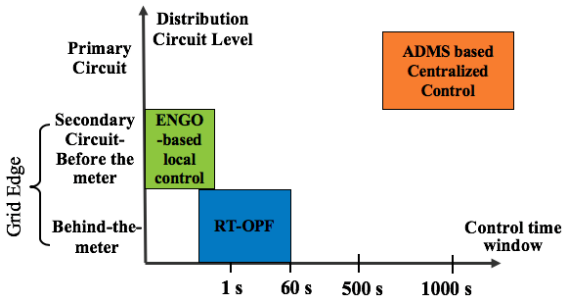

Fig. 3. Coordination among the three control timescales.

III. Use Case Study

To evaluate the DEHC architecture, analytical simulations are performed to study both the feasibility and effectiveness of the DEHC architecture using a co-simulation framework that is developed by the authors using Python language and OpenDSS [9] software simulation. Distribution feeder and PV systems are modeled using OpenDSS, and the ENGO device is modeled by Varentec using a DLL file. Although ENGO local response time is subcycle in real field application, the DLL file model can only alter its reactive power output every one second. To address the mismatch between actual response time and simulated ENGO model response time, we perform the simulation study with 1 second time step, but have expanded the simulation horizon into eight times longer, so that 1 second simulation time is considered as 1/8 second real time. And both load demands and PV generations are interpolated appropriately to meet the requirement.

A. Distribution Feeder Information

A real distribution feeder provided by our utility partner, Xcel Energy, is modeled using OpenDSS to test the performance of the DEHC architecture. This feeder has 4,952

nodes and serves 1,348 customers. Fig. 4 shows the feeder topology, plotted using the GridPV tool [10], which includes the locations of the substation LTC, capacitor banks (nonswitchable), ENGO devices, and PV inverters.

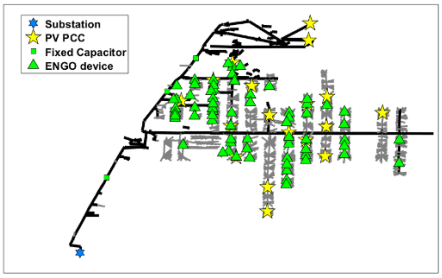

Fig. 4. Topology of the studied distribution feeder.

To fully consider the effect of solar intermittency on distribution system operation, we selected a day with highly fluctuating solar irradiance to conduct quasi-static time-series (QSTS) simulations. Fig. 5 shows 1-day load and PV profiles used in the simulation study.

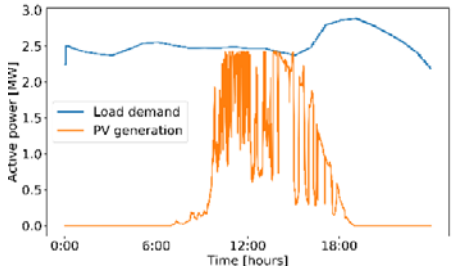

Fig. 5. One-day load and PV profiles used for QSTS simulation.

B. Simulation Results

The feeder response is studied using the following four scenarios:

1. Baseline scenario (S1): In the baseline scenario, the ENGO devices are disabled. The PV systems are assumed to be supplying power at unity power factor.
2. Scenario 2 (S2): The ENGO devices are in service in this scenario and are operating with a fixed voltage-regulation set point of 1.033 p.u., which is the same as the LTC set point.
3. Scenario 3 (S3): The PV systems are dispatched using the RT-OPF in this scenario, and the ENGO devices are not present.
4. Scenario 4 (S4): The RT-OPF dispatch of the PV systems is employed while the ENGO devices are in service.

1) Baseline Scenario (S1)

The feeder voltage profile at the peak load snapshot simulation in the baseline scenario is shown in Fig. 6, highlighting the PV and fixed capacitor locations. In this figure, the solid lines represent the line voltage drops of the primary distribution system, and the dashed lines represent the voltage drops in the low-voltage secondary network. Many secondary buses are experiencing high-voltage violations with voltages exceeding 1.05 p.u. primarily because of the presence of excessive levels of PV generation in this scenario.

To further study the baseline feeder response, the QSTS simulation is performed for a 24-hour period with 1-second time step resolution. The maximum and minimum voltages in the system (V_{max} and V_{min}) during the simulated day are shown in Fig. 7. In addition to the high-voltage, long-sustaining violations between the hours 10 and 18, voltage volatility resulting from PV power output intermittencies is evident in this figure. These voltage issues need to be addressed by exercising advanced controls.

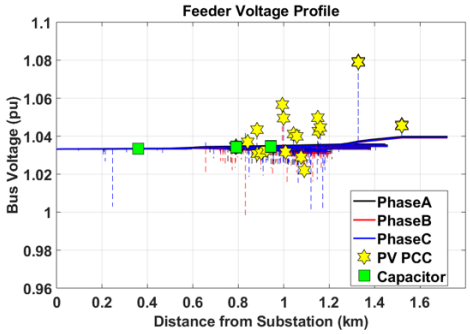

Fig. 6. Baseline feeder voltage profile.

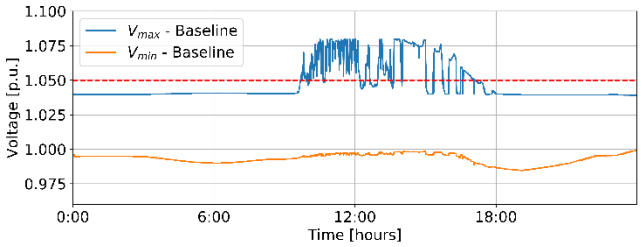

Fig. 7. Maximum and minimum voltages in the feeder on simulated day.

2) Scenario 2 (S2)

In this scenario, the ENGO devices are enabled and are configured to regulate the voltages at their terminals at 1.033 p.u. Voltage regulation is achieved by dynamic adjustment of reactive power support by the ENGOs.

The extreme voltages in the feeder recorded from the QSTS simulation are shown in the upper graph of Fig. 8 along with the voltages observed in the S1 for comparison. Compared to the baseline, the minimum voltage in this scenario is increased because of the dynamic capacitive reactive power support from the ENGO devices. Further, no change is observed in the maximum feeder voltage during the entire simulated day. Because the ENGO devices dynamically reduce their power output when their terminal voltages are rising beyond the voltage set point, they do not create overvoltage issues in the system even when numerous devices are installed. The total reactive power injection from all the ENGO devices (Q_{total_ENGO}) is shown in the bottom graph of Fig. 8, which highlights the dynamic behavior of the ENGO devices. The total reactive power from these devices is reduced during the peak PV generation period. The average voltage at all the ENGO connected nodes in S2 (V_{ENGO_avg} – S2) is compared with that of the baseline scenario (V_{ENGO_avg} – Baseline) in Fig. 7 to highlight the voltage boost by the ENGOs.

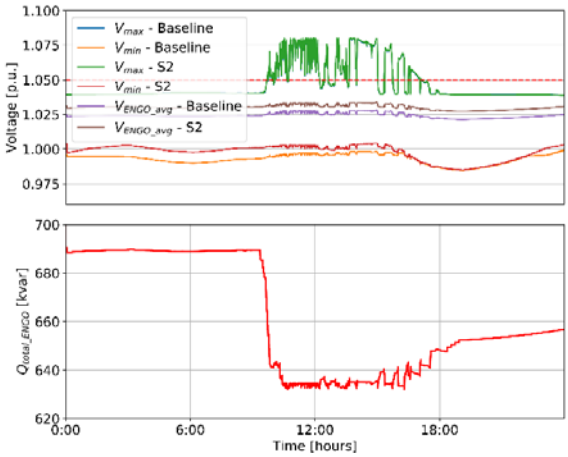

Fig. 8. Voltage boost provided by ENGO devices through dynamic reactive power injection.

3) *Scenario 3 (S3)*

The PV systems are dispatched using RT-OPF in this scenario. To study the impact of the RT-OPF acting alone on the feeder voltage profile, the ENGO devices are disabled. The feeder's extreme voltages and the total PV generation in this scenario are compared to the same quantities of S1 in Fig. 9. During the period when highly intermittent PV generation is present, between the hours 10 and 18, reactive power is dispatched from the PV inverters to regulate the system voltages within operational limits. When the reactive power dispatch alone is insufficient for the voltage regulation, active power curtailment occurred; however, it is evident that the active power curtailment is minimal.

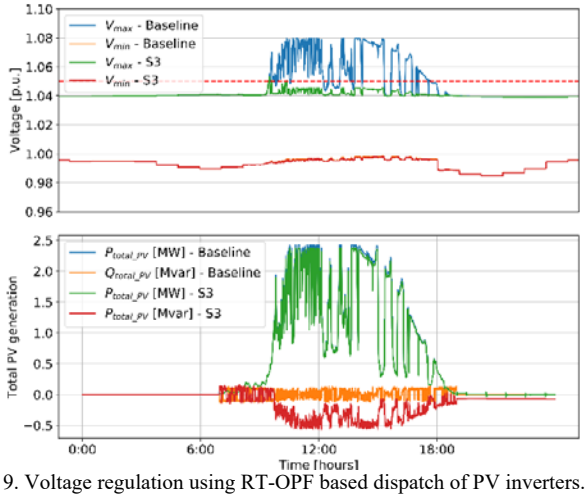

Fig. 9. Voltage regulation using RT-OPF based dispatch of PV inverters.

1) *Scenario 4 (S4)*

The impact of both RT-OPF based dispatch of PV systems and the dynamic reactive power support by the ENGO devices acting together is studied in S4. The extreme voltages and the real and reactive power supply from the PV systems and ENGO devices are shown in Fig. 10. For comparison, the results from S3 are also plotted. The mitigation of high-voltage violations as result of reactive power absorption by the PV inverters and voltage boost caused by capacitive reactive power supply by the ENGO devices are observed in this scenario.

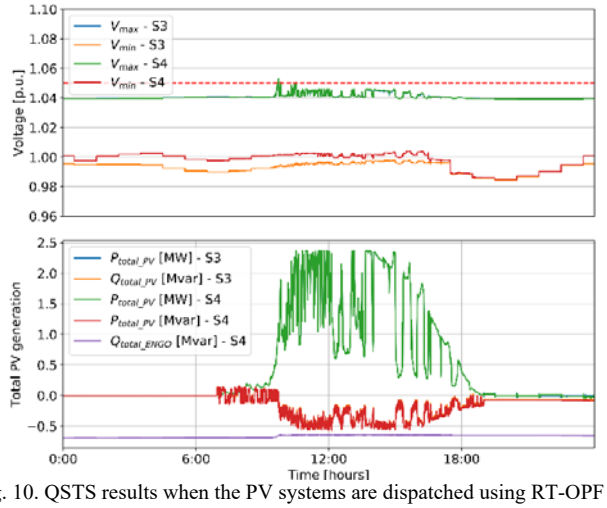

Fig. 10. QSTS results when the PV systems are dispatched using RT-OPF in the presence of ENGO devices.

IV. Conclusions and Acknowledgement

A novel data-enhanced hierarchical control is presented in this paper, and its feasibility and effectiveness are briefly demonstrated based on four scenario simulation studies. More work will be completed in the future to comprehensively demonstrate the effectiveness of the architecture to provide multiscale grid operation benefits.

This work is funded by the DOE under the Enabling Extreme Real-time Grid Integration of Solar Energy (ENERGISE) program. The authors would like to thank the support from our project partners, including Schneider Electric, Varentec, Xcel Energy, and EPRI.

References

[1] Y. Liu, J. Bebic, B. Kroposki, J. de Bedout, and W. Ren, "Distribution system voltage performance analysis for high-penetration PV," in *IEEE Energy 2030 Conf.*, Nov. 2008.

[2] Woyte, V. Van Thong, R. Belmans and J. Nijs, "Voltage fluctuations on distribution level introduced by photovoltaic systems," *IEEE Transactions on Energy Conversion*, vol. 21, no. 1, pp. 202-209, March 2006.

[3] ANSI C84.1-2016, "American National Standard for Electric Power Systems and Equipment – Voltage Ratings (60 Hz)", National Electrical Manufactures Association.

[4] https://www.schneider-electric.com/en/work/solutions/for business/s4/electric-utilities-advanced-distribution-management-system-adms/.

[5] R. Moghe, D. Tholomier, D. Divan, J. Schatz and D. Lewis, "Grid edge control: a new approach for volt-var optimization," *in 2016 IEEE PES Transmission and Distribution Conference and Exposition (T&D)*, Dallas, TX, USA, May 2016.

[6] D. Divan, R. Moghe and H. Chun, "Managing distribution feeder voltage issues caused by high PV penetration," *in 2016 IEEE 7th International Symposium on Power Electronics for Distributed Generation Systems (PEDG)*, Canada, June 2016.

[7] Dall'Anese and A. Simonetto, "Optimal Power Flow Pursuit," *IEEE Trans. on Smart Grid*, vol. 9, no. 2, pp. 942-952, March 2018.

[8] A. Bernstein and E. Dall'Anese, "Linear power flow models in multiphase distribution networks," *in 2017 IEEE PES Innovative Smart Grid Technologies Conference Europe (ISGT-Europe)*, Italy, Sep. 2017.

[9] http://smartgrid.epri.com/SimulationTool.aspx.

[10] M. J. Reno and K. Coogan, "Grid Integrated Distributed PV (GridPV) Version 2," Sandia National Laboratories SAND2014-20141, 2014.